Joint Modeling of fMRI and EEG Imaging Using Ordinary Differential Equation-Based Hypergraph Neural Networks

Yan Zhang, Yang Gao, Min Li*
School of Computer Science and Engineering
Central South University
Changsha, Hunan 410083
limin@mail.csu.edu.cn

Abstract

Fusing multimodal brain imaging has been a hot topic since different modalities of brain imaging can provide complementary information. However, due to the size of simultaneous recorded fMRI-EEG dataset being limited and the substantial discrepancy between hemodynamic responses of fMRI and neural oscillations of EEG, the joint modeling of fMRI and EEG images is a rarely explored area and has not yielded satisfactory results. Existing studies have also indicated that the relationships between region of interest (ROI) are not one-to-one when synchronizing fMRI and EEG. Current graph-based multimodal modeling methods overlook those information. Based on this, we propose a hypergraph based fMRI-EEG modeling framework for asynchronous fMRI-EEG data named FE-NET. To the best of our knowledge, this is the first attempt to jointly model asynchronous EEG and fMRI data as Neural ODEs based hypergraph. Extensive experiments have demonstrated that the proposed FE-NET outperforms many state-of-the-art brain imaging modeling methods. Meanwhile, compared to simultaneously recorded fMRI-EEG data, asynchronously acquired fMRI-EEG data is less costly, which demonstrates the practical applicability of our method.

1 Introduction

A major goal in neuroimaging research is to develop predictive models aimed at analyzing the association between comprehensive functional connectivity patterns across the brain and behavioral traits, which can enhance the understanding of both normal brain function and dysfunction [1]. A robust modeling method plays a significant role in assisting the diagnosis of neurological disorders, predicting infant neurodevelopment, and assessing sleep quality [2; 3; 4]. Usually, researchers model brain imaging in the form of graphs to accomplish this goal [5].

In recent years, modeling multimodal brain imaging has emerged as a focal point of research. fMRI indirectly measures brain activity through the Blood Oxygen Level Dependent (BOLD) signal, while EEG directly records brain activity by measuring the electric fields generated by cortical pyramidal neurons. EEG enables non-invasive observation of brain electrical activity and serves as a complementary modality to fMRI:

The integration of fMRI with EEG signals offers a promising approach to bridging the gap between hemodynamic responses and neural oscillations, providing insights into the origins of fMRI signals and their large-scale patterns. However, deep learning-based joint modeling of asynchronously recorded fMRI and EEG is a relatively underexplored area and has not yielded satisfactory results.

*Corresponding author.

39th Conference on Neural Information Processing Systems (NeurIPS 2025).

The reasons for this issue are twofold. One reason lies in the incompatibility of the equipment, the sample size of simultaneously recorded fMRI-EGG datasets is markedly smaller than that of asynchronously acquired datasets, thereby limiting the reliability of extant research relying on synchronous recordings, another reason is the fundamental differences of the signal type make the data distribution between fMRI and EEG highly complex, thereby rendering it difficult to bridge the gap between them.

Existing studies [6] have indicated that the relationships between regions of interest (ROI) are not one-to-one when synchronizing fMRI and EEG, Hyperedges in hypergraphs can connect multiple nodes, providing a more comprehensive description of this relationship.

Neural ordinary differential equations (Neural ODEs) [7] can dynamically propagate information across arbitrary timestamps, accommodating mismatched sampling rates and asynchronous time points without manual alignment, the potential of using Neural ODEs for modeling asynchronous data has been widely reported [8].

Based on the existing issues, we propose a fMRI-EEG modeling method based on Neural ODEs hypergraphs. Our main innovations are as follows:

1) We have designed a GAN-based fMRI-EEG hypergraph generation (FEH) module, which employs a novel Optimal fMRI-EEG Isomorph algorithm (OFEI) and Interactive Hyperedge Neurons (IHEN) to generate multiple hypergraphs at various temporal and spatial scales. The strength of GAN-based FEH lies in their ability to learn the complex data distribution between fMRI and EEG through synchronized operation of OFEI and IHEN, thus narrowing the gap between the hemodynamic responses and the neural oscillations.

2) We proposed a novel dynamic fMRI-EEG hypergraph embedding module (FED), which leverages Neural ODEs to capture latent temporal dependencies between fMRI's slow hemodynamic changes (s̃econds) and EEG's rapid neural oscillations (m̃illiseconds), Neural ODEs naturally handles inconsistency sampling rates and temporal mismatches by learning differential equations governing system dynamics for asynchronous data.

3) To the best of our knowledge, this is the first attempt to model asynchronous EEG and fMRI data as Neural ODEs based hypergraph. Comprehensive experiments show that the performance of the proposed FE-NET surpasses many state-of-the-art methods, compared to simultaneously recorded fMRI-EEG data. Asynchronously acquired fMRI-EEG data is less costly, which demonstrates the practical applicability of our method.

2 Related Work

2.1 Hypergraph Learning

In recent years, the efficacy of hypergraphs in modeling and comprehending intricate correlations has become evident. Initially introduced by [9], hypergraph learning embodies a transductive learning approach, conceptualized as a dissemination process within the hypergraph structure.

Motivated by the remarkable success of deep learning, some researchers have ventured into developing deep hypergraph learning techniques. For instance, Feng et al. [10] introduced hypergraph neural networks (HGNN) to model and understand beyond-pairwise intricate correlations. Unlike Graph Neural Networks (GNN), HGNN devises a vertex-hyperedge-vertex information propagation schema to iteratively glean data representation. Bai et al. [11] delved deeper into the attention mechanism on hypergraphs, aligning with the hypergraph convolution paradigms delineated in HGNN. Inspired by [12], Hyper-Atten introduces a hyperedge-vertex attention learning module to dynamically discern the importance of different vertices within the same hyperedge, thereby unveiling intrinsic correlations. Moreover, Yadati et al. [13] proposed HyperGCN, a method for training a Graph Convolutional Network (GCN) on hypergraphs for semi-supervised learning. HyperGCN is structured based on the spectral theory of hypergraphs. Initially, HyperGCN transforms a hypergraph into a simple weighted graph via a specific strategy and subsequently executes standard GCN on the graph to glean data representations.

As elucidated, most prevailing deep hypergraph learning methods stem from the spectral theory of hypergraphs. Consequently, these methods are typically defined on static hypergraphs system, constraining their applications. Failing to capture the continuous evolution of fMRI-EEG hypergraph

representations. Many important information in the dynamic continuous representations between fMRI and EEG has been lost.

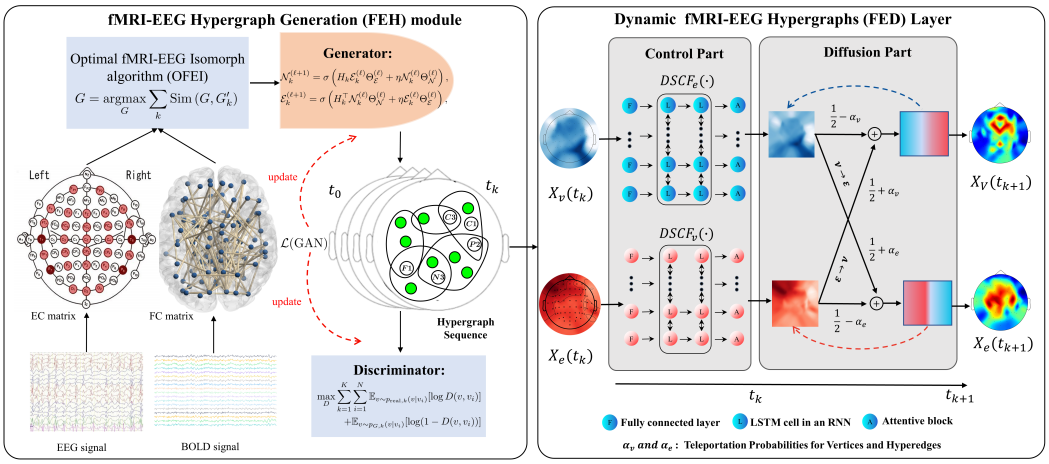

Figure 1: Overall process of GAN-based hypergraph generation (FEH) module and Dynamic hypergraphs embedding (FED) module.

3 Method

As shown in Figure 1, our method consists of two steps. Firstly, multiple fMRI-EEG hypergraphs are generated at various temporal and spatial scales by GAN-based fMRI-EEG hypergraph generation module. Then, these hypergraphs are inputted into the dynamic fMRI-EEG hypergraph embedding module.

3.1 Preliminary

Notations. In the hypergraph, each hyperedge, which is a subset of the vertex set, exhibits a distinction from the simple graph. Typically, a hypergraph is defined as $\mathcal{G} = (\mathcal{V}, \mathcal{E})$, where $\mathcal{V}$ and $\mathcal{E}$ denote the vertex set and hyperedge set, respectively. The hyperedges are represented by an incidence matrix $\boldsymbol{H} \in \{0,1\}^{|\mathcal{V}|\times|\mathcal{E}|}$, with its elements defined as $H_{v,e} = \mathbf{1}(\mathrm{v} \in \mathrm{e})$ utilizing the indicator function $1(\cdot)$. The degree of a vertex $v \in \mathcal{V}$ is determined by the summation of the hyperedge occurrences $H_{v,e}$ over the hyperedge set $\mathcal{E}$, denoted as $d(v) = \sum_{e\in\mathcal{E}} H_{v,e}$. Similarly, the degree of a hyperedge $e \in \mathcal{E}$ is determined by the summation of the vertex occurrences $H_{v,e}$ over the vertex set $\mathcal{V}$, denoted as $\delta(e) = \sum_{v\in\mathcal{V}} H_{v,e}$. The diagonal degree matrices for vertices and hyperedges are represented as $\boldsymbol{D}_v = \mathrm{diag}(\boldsymbol{d})$ and $\boldsymbol{D}_e = \mathrm{diag}(\boldsymbol{\delta})$, respectively.

Hypergraph neural networks. The majority of contemporary hypergraph neural networks adhere to the message-passing framework. Within each layer, the input vertex representations are initially aggregated into hyperedges, and subsequently, the output vertex representations are derived from the corresponding hyperedges. Formally, in the k-th layer, the output vertex representations $\boldsymbol{x}_v^{(k)}$ are computed based on the previous representations through the employment of the aggregation function AGG and the update function UPD as follows:

$$\boldsymbol{x}_v^{(k)} = \mathrm{UPD}\left(\boldsymbol{x}_v^{(k-1)}, \mathrm{AGG}\left(\left\{\boldsymbol{x}_e^{(k)} : e \in \mathcal{N}_e(v)\right\}\right)\right), \quad \boldsymbol{x}_e^{(k)} = \mathrm{AGG}\left(\left\{\boldsymbol{x}_v^{(k-1)} : v \in \mathcal{N}_v(e)\right\}\right) \tag{1}$$

where $\mathcal{N}_e(v)$ and $\mathcal{N}_v(e)$ correspond to the vertex and hyperedge neighbor functions, respectively.

3.2 GAN-based fMRI-EEG hypergraph generation (FEH) module

3.2.1 Optimal fMRI-EEG Isomorph algorithm (OFEI)

As shown in Figure 1 (left), each region of interest (ROI) is conceptualized as a node within the framework. Initially, the Dynamic Hypergraph Construction algorithm (DHC) defined in [14], is

employed to compute the initial hypergraphs $\{G'_k\}_{k=1}^{t}$ for each subject within the dataset, where t represents the aggregate number of samples. If these initial hypergraphs $\{G'_k\}$ are directly utilized in the generative process to achieve multimodal connectivity, the robustness of the resultant generation may be compromised. In response to this limitation, we design a novel Optimal fMRI-EEG Isomorph algorithm (OFEI), which is capable of calculating a hypergraph G that exhibits optimal isomorphism relative to the initial hypergraphs $\{G'_k\}$,

Let $G = (V, E)$ and $G' = (V, E')$ share the same vertex set and have the same number of hyperedges, $m = |E| = |E'|$. Index the edges as $E = \{e_1, \ldots, e_m\}$ and $E' = \{e'_1, \ldots, e'_m\}$. For an edge e, let $\mathcal{V}_G(e) \subseteq V$ denote its incident-vertex set. Define the edge-wise Jaccard similarity

$$s(e, e') = \frac{|\mathcal{V}_G(e) \cap \mathcal{V}_{G'}(e')|}{|\mathcal{V}_G(e) \cup \mathcal{V}_{G'}(e')|}. \tag{2}$$

The homogeneity between G and G' is

$$\mathrm{Sim}(G, G') := \max_{\sigma \in S_m} \frac{1}{m} \sum_{i=1}^{m} s\big(e_i, e'_{\sigma(i)}\big), \tag{3}$$

i.e., the maximum over bijections $f : E \to E'$ (since $|E| = |E'|$).

Writing $\mathcal{H}(V, m)$ for the class of hypergraphs on V with m hyperedges, OFEI solves

$$G^* \in \arg \max_{G \in \mathcal{H}(V,m)} \sum_{k=1}^{t} \mathrm{Sim}\left(G, G'_k\right). \tag{4}$$

With the optimal isomorph G^* in hand, we construct subject-specific hypergraphs by concatenating G^* with each G'_k,

$$G_k := G^* \,\|\, G'_k, \tag{5}$$

where $\|$ denotes edgewise concatenation on the common vertex set (allowing multiplicities if applicable). The corresponding incidence matrices are then obtained as

$$H_k = H(G_k) \quad \text{(equivalently, } H_k = [\, H(G^*) \,\big|\, H(G'_k)\,]\text{)}. \tag{6}$$

The rationale behind OFEI lies in its ability to establish a metric for measuring the similarity among hypergraphs, thereby enhancing the correlation between fMRI and EEG data. This ensures the generated hypergraph preserves the topological consistency of brain connectivity across modalities,the data alignment and node correspondence part are provided in supplementary material.

3.2.2 Generator formed by interactive hyperedge neurons module

For the k-th participant, we initialize node representations $\mathcal{N}_k^{(0)} \in \mathbb{R}^{N \times d}$ directly from their BOLD signal matrix B_k, where N denotes the ROI count and d the temporal length. Simultaneously, hyperedge representations $\mathcal{E}_k^{(0)} \in \mathbb{R}^{m \times N}$ are constructed via $\mathcal{E}_k^{(0)} = H_k^\top S_k$, where $S_k \in \mathbb{R}^{N \times N}$ is the effective connectivity matrix, $H_k \in \mathbb{R}^{N \times m}$ is the incidence structure, and m represents the hyperedge cardinality.

The generative architecture $\mathcal{G}$ consists of L cascaded Interactive Hyperedge Neuron (IHEN) transformations. For layer index $\ell \in \{0, 1, \ldots, L-1\}$, the IHEN propagation rules are:

$$\mathcal{N}_k^{(\ell+1)} = \sigma\left(H_k \mathcal{E}_k^{(\ell)} \Theta_{\mathcal{E}}^{(\ell)} + \eta \mathcal{N}_k^{(\ell)} \Theta_{\mathcal{N}}^{(\ell)}\right), \mathcal{E}_k^{(\ell+1)} = \sigma\left(H_k^\top \mathcal{N}_k^{(\ell)} \Theta_{\mathcal{N}}^{(\ell)} + \eta \mathcal{E}_k^{(\ell)} \Theta_{\mathcal{E}}^{(\ell)}\right), \tag{7}$$

where $\Theta_{\mathcal{N}}^{(\ell)}$ and $\Theta_{\mathcal{E}}^{(\ell)}$ are learnable transformation matrices for nodes and hyperedges respectively, and η is a mixing coefficient.

From the terminal representations $\mathcal{N}_k^{(L)}$ and $\mathcal{E}_k^{(L)}$, we compute node-to-hyperedge affinities and hyperedge importances. Define the affinity of node v_i to hyperedge e_j as:

$$\phi_{k,j}(i) = H_k(i, j) \cdot \langle \mathcal{N}_k^{(L)}[i, :], \mathcal{E}_k^{(L)}[j, :] \rangle, \tag{8}$$

and the importance weight of hyperedge e_j as:

$$\omega_k(j) = \left\| \mathcal{E}_k^{(L)}[j, :] \right\|_2. \tag{9}$$

The multimodal connectivity tensor $\mathcal{M}_k \in \mathbb{R}^{N\times N}$ is then assembled via:

$$\mathcal{M}_k[p,q] = \sum_{j=1}^{m} \omega_k(j) \cdot \phi_{k,j}(p) \cdot \phi_{k,j}(q). \tag{10}$$

Finally, node-wise correlation scores are computed by integrating connectivity strengths with feature similarities:

$$\mathcal{C}_k(i) = \frac{1}{N} \sum_{q=1}^{N} \mathcal{M}_k[i,q] \cdot \langle \mathcal{N}_k^{(L)}[i,:], \mathcal{N}_k^{(L)}[q,:] \rangle. \tag{11}$$

3.2.3 Discriminator and Loss Function

The discriminator $\mathcal{D}$ utilizes a standard multilayer perceptron architecture. Given an arbitrary initial node u_0, we initiate random walks from this origin. For a walk of length T terminating at u_T, the traversal sequence $\mathbf{u} = (u_0, u_1, \ldots, u_{T-1}, u_T, u_{T+1})$ satisfies the boundary condition $u_{T+1} = u_{T-1}$, establishing u_T as the terminal node.

For the functional connectivity matrix $\mathbf{F}_k$ of subject k, the probability of realizing trajectory $\mathbf{u}$ is:

$$P_k^{\text{emp}}(\mathbf{u}) = \prod_{i=1}^{T} \frac{\mathbf{F}_k(u_{i-1}, u_i)}{\sum_j \mathbf{F}_k(u_{i-1}, j)} \times \frac{\mathbf{F}_k(u_T, u_{T-1})}{\sum_j \mathbf{F}_k(u_T, j)} \tag{12}$$

Denoting $\Omega(u_0 \to v)$ as the collection of all paths from u_0 to destination v, the marginal probability is:

$$P_k^{\text{emp}}(v \mid u_0) = \sum_{\gamma \in \Omega(u_0 \to v)} P_k^{\text{emp}}(\gamma) \tag{13}$$

For the generated multimodal connectivity matrix $\mathbf{M}_k$, the corresponding trajectory probability becomes:

$$P_k^{\text{gen}}(\mathbf{u}) = \prod_{i=1}^{T} \frac{\mathbf{M}_k(u_{i-1}, u_i)}{\sum_j \mathbf{M}_k(u_{i-1}, j)} \times \frac{\mathbf{M}_k(u_T, u_{T-1})}{\sum_j \mathbf{M}_k(u_T, j)} \tag{14}$$

with marginal distribution:

$$P_k^{\text{gen}}(v \mid u_0) = \sum_{\gamma \in \Omega(u_0 \to v)} P_k^{\text{gen}}(\gamma) \tag{15}$$

The discriminator objective function is formulated as:

$$\mathcal{L}_{\mathcal{D}} = \max_{\mathcal{D}} \sum_{k=1}^{K} \sum_{n=1}^{N} \left[\mathbb{E}_{v \sim P_k^{\text{emp}}(\cdot \mid u_n)} [\log \mathcal{D}(v, u_n)] + \mathbb{E}_{v \sim P_k^{\text{gen}}(\cdot \mid u_n)} [\log(1 - \mathcal{D}(v, u_n))] \right] \tag{16}$$

where K represents the cohort size and N the number of nodes.

The generator objective, driven by discriminator feedback, is:

$$\mathcal{L}_{\mathcal{G}} = \max_{\mathcal{G}} \sum_{k=1}^{K} \sum_{n=1}^{N} \mathbb{E}_{v \sim P_k^{\text{gen}}(\cdot \mid u_n)} [\log \mathcal{D}(v, u_n)] \tag{17}$$

The OFEI framework achieves optimal structural correspondence across multimodal fMRI-EEG hypergraph representations, while the IHEN mechanism dynamically modulates hyperedge weights $\phi_{k,j}(i)$ through learned node-hyperedge affinities, emphasizing neurobiologically significant connectivity patterns (e.g., functionally coherent brain networks).

The FEH module combines **structural optimization** (OFEI), **dynamic feature fusion** (IHEN), and **distribution alignment** (GAN) to generate hypergraphs that bridge fMRI and EEG's gaps at various temporal and spatial scales, thus can narrow the gap between the hemodynamic responses and the neural oscillations, subsequently, fMRI-EEG hypergraphs will be sent into the dynamic FMRI-EEG hypergraphs embedding module for feature extraction.

3.3 Dynamic fMRI-EEG hypergraphs embedding (FED) module

In this section, we first give the definition of dynamic fMRI-EEG hypergraph systems and provide a specific dynamic fMRI-EEG hypergraph systems based on ODE. Next, we describe the detailed neural implementation of the FED $^{\text{ode}}$ framework, the overall process of FED module is shown in Figure 1.

3.3.1 Definition of dynamic fMRI-EEG hypergraph systems

Given a hypergraph $\mathcal{G}$, a corresponding vertex feature matrix $\boldsymbol{Z}_v \in \mathbb{R}^{|\mathcal{V}|\times c}$, and a corresponding hyperedge feature matrix $Z_e \in \mathbb{R}^{|\mathcal{E}|\times c}$, our goal is to learn a vertex representation $\boldsymbol{Y}_v$ and a hyperedge representation $\boldsymbol{Y}_e$. We first define dynamic fMRI-EEG hypergraph systems based on the following equation:

$$\begin{bmatrix} \dot{\boldsymbol{X}}_v \\ \dot{\boldsymbol{X}}_e \end{bmatrix} = f\left(\begin{bmatrix} \boldsymbol{X}_v(t) \\ \boldsymbol{X}_e(t) \end{bmatrix}\right) \text{ and } \begin{bmatrix} \boldsymbol{X}_v(0) \\ \boldsymbol{X}_e(0) \end{bmatrix} = \begin{bmatrix} \boldsymbol{Z}_v \\ \boldsymbol{Z}_e \end{bmatrix} \tag{18}$$

Here, $\boldsymbol{X}_v(t)$ and $\boldsymbol{X}_e(t)$ denote the matrices representing vertex and hyperedge features at time t, respectively. The function f encapsulates the rate of change within the dynamic system, with $\boldsymbol{Z}_v$ and $\boldsymbol{Z}_e$ representing the initial conditions for vertex and hyperedge features, respectively. The persistence of timestamp t allows the hypergraph dynamic systems to continuously update representation states.

ODE-based hypergraph dynamic system. The velocity function f in Equation(18) may be characterized variably. It is proposed to interpret the velocity function as a composite of a control function and a diffusion function, thereby formulating an ODE-based hypergraph dynamic system in the following manner:

$$\begin{bmatrix} \dot{\boldsymbol{X}}_v \\ \dot{\boldsymbol{X}}_e \end{bmatrix} = \begin{bmatrix} C_v\left(\boldsymbol{X}_v(t)\right) \\ C_e\left(\boldsymbol{X}_e(t)\right) \end{bmatrix} + \boldsymbol{H}\begin{bmatrix} \boldsymbol{X}_v(t) \\ \boldsymbol{X}_e(t) \end{bmatrix}. \tag{19}$$

In the initial segment of the equation, C_v and C_e serve as control functions, which correspond to the velocity of control for the representations of vertices and hyperedges, respectively. The subsequent segment represents the diffusion term.

$$\begin{bmatrix} \boldsymbol{X}_v(T) \\ \boldsymbol{X}_e(T) \end{bmatrix} = \begin{bmatrix} \boldsymbol{X}_v(0) \\ \boldsymbol{X}_e(0) \end{bmatrix} + \int_0^T C\left(\begin{bmatrix} \boldsymbol{X}_v(t) \\ \boldsymbol{X}_e(t) \end{bmatrix}\right) dt \tag{20}$$

Given the initial vertex features $\boldsymbol{X}_v(0)$ and hyperedge features $\boldsymbol{X}_e(0)$ as inputs, the corresponding vertex representations $\boldsymbol{X}_v(T)$ and hyperedge representations $\boldsymbol{X}_e(T)$ at time T are generated through integration, as outlined in Equation(20), for learning tasks within the hypergraph.

We anticipate proposing a multi-layer neural network framework, denoted as FED$^{\text{ode}}$. Initially, we adopt the Lie-Trotter splitting method, as delineated by Geiser [15], for the discretization of Equation(19), delineated below:

$$\begin{aligned} \begin{bmatrix} \boldsymbol{X}_v\left(t+\frac{1}{2}\right) \\ \boldsymbol{X}_e\left(t+\frac{1}{2}\right) \end{bmatrix} &= \begin{bmatrix} \boldsymbol{X}_v(t) \\ \boldsymbol{X}_e(t) \end{bmatrix} + \begin{bmatrix} C_v\left(\boldsymbol{X}_v(t)\right) \\ C_e\left(\boldsymbol{X}_e(t)\right) \end{bmatrix}, \\ \begin{bmatrix} \boldsymbol{X}_v(t+1) \\ \boldsymbol{X}_e(t+1) \end{bmatrix} &= \begin{bmatrix} \boldsymbol{X}_v\left(t+\frac{1}{2}\right) \\ \boldsymbol{X}_e\left(t+\frac{1}{2}\right) \end{bmatrix} + \boldsymbol{A}\begin{bmatrix} \boldsymbol{X}_v\left(t+\frac{1}{2}\right) \\ \boldsymbol{X}_e\left(t+\frac{1}{2}\right) \end{bmatrix}, \end{aligned} \tag{21}$$

In the model, the time step is incorporated into control functions C_v and C_e, as well as the diffusion matrix $\boldsymbol{A}$. Lie-Trotter discretization strategy allow separates control (modality-specific dynamics) part and diffusion (cross-modal interactions) part, allowing asynchronous updates of fMRI and EEG features while preserving their intrinsic temporal characteristics.

3.3.2 Neural implementation of the FED $^{\text{ode}}$ framework

we delineate the integration of the FED$^{\text{ode}}$ framework into the antecedent analysis by elucidating the neural instantiation of both the control and diffusion phases within the FED$^{\text{ode}}$ layer, separately. A graphical representation of the FED$^{\text{ode}}$ framework is provided in Figure 1 (right).

Neural implementation of control step. To extract spatio-temporal information from fMRI and EEG data, we propose a Dual-Stream Control Function (DSCF). As illustrated in Figure 1, DSCF incorporates components where F, L, and A represent, respectively, a fully connected layer, an LSTM

cell in an RNN, and an attentive block aligned with an RNN output defined in literature [16]. The control function of FED $^{\text{ode}}$ layer is specifically articulated through the subsequent equation:

$$\begin{bmatrix} \boldsymbol{X}_v\left(t+\frac{1}{2}\right) \\ \boldsymbol{X}_e\left(t+\frac{1}{2}\right) \end{bmatrix} = \begin{bmatrix} \boldsymbol{X}_v(t) \\ \boldsymbol{X}_e(t) \end{bmatrix} + \begin{bmatrix} DSCF_v(\boldsymbol{X}_v(t)) \\ DSCF_e(\boldsymbol{X}_e(t)) \end{bmatrix} \tag{22}$$

In this study, the temporal dynamics of brain activity can convey essential information. Therefore, using a LSTM to capture the spectral variations within the activation sequence of networks is a rational approach. The Attention Neural Network (ANN) [17] applies distinct weights to various output steps of RNNs to prioritize the most critical time periods, thereby playing a crucial role in subject-independent hypergraph encoding. Input and output parameters for FN, LSTM, and ANN are provided in the Supplementary Material.

Neural implementation of diffusion step. The configuration of the diffusion matrix $\boldsymbol{A}$ is paramount. Should it be improperly formulated, both vertex and hyperedge representations are prone to diverge and become intractable, delineated as follows:

$$\begin{aligned} \begin{bmatrix} \boldsymbol{X}_v(t+1) \\ \boldsymbol{X}_e(t+1) \end{bmatrix} &= \begin{bmatrix} \frac{1}{2}\boldsymbol{X}_v\left(t+\frac{1}{2}\right) \\ \frac{1}{2}\boldsymbol{X}_e\left(t+\frac{1}{2}\right) \end{bmatrix} + \boldsymbol{A} \begin{bmatrix} \boldsymbol{X}_v\left(t+\frac{1}{2}\right) \\ \boldsymbol{X}_e\left(t+\frac{1}{2}\right) \end{bmatrix} \\ \boldsymbol{A} &= \begin{bmatrix} -\alpha_v \boldsymbol{I} & (\frac{1}{2}+\alpha_v)\boldsymbol{D}_v^{-1}\boldsymbol{H} \\ (\frac{1}{2}+\alpha_e)\boldsymbol{D}_e^{-1}\boldsymbol{H}^\top & -\alpha_e \boldsymbol{I} \end{bmatrix}, \end{aligned} \tag{23}$$

In the context where α_v and α_e serve as hyperparameters, these denote the teleportation probabilities associated with vertices and hyperedges, respectively. We proceed to decompose the matrix multiplication term to derive the vertex representation: $\boldsymbol{X}_v(t+1) = \left(\frac{1}{2}-\alpha_v\right)\boldsymbol{X}_v\left(t+\frac{1}{2}\right) + (\frac{1}{2}+\alpha_v)\boldsymbol{D}_v^{-1}\boldsymbol{H}\boldsymbol{X}_e\left(t+\frac{1}{2}\right)$. Here, the initial term indicates that vertex representations are maintained with a preservation factor of $\frac{1}{2}-\alpha_v$ during the diffusion process, while the latter term signifies the integration of representations from hyperedges directly linked to each vertex, weighted by α_v. In this arrangement, $\boldsymbol{H}\boldsymbol{X}_e\left(t+\frac{1}{2}\right)$ corresponds to vertex-level aggregation, and $\boldsymbol{D}_v^{-1}$ serves as a normalization matrix for averaging.

Control part in FEH refine modality-specific features (i.e., isolating fMRI spatial patterns from EEG spectral power). The Diffusion part can propagates information across the hypergraph structure, capturing long-range dependencies (i.e., cross-modal interactions between distant brain regions and transient EEG signals). The control-diffusion mechanism in FEH ensures that hypergraph representations evolve smoothly over time , mimicking the gradual emergence of stable brain states.

4 Experiments

4.1 Data and Pre-processing

The fMRI-EEG dataset we used is LEMON, which is open access and was referenced in the literature [18], encompasses data from 227 healthy participants. This cohort includes a young group (N=153, age 25.1±3.1 years, range 20–35 years, 45 females) and an elderly group (N=74, age 67.6±4.7 years, range 59–77 years, 37 females). Participants underwent resting-state fMRI and a 62-channel EEG experiment. The preprocessing protocol for rs-fMRI data was conducted utilizing the Nipype framework as defined in [18]. Data preprocessing procedures for EEG were executed utilizing EEGLAB105 (version 14.2.1b) [19]. The preprocessing entailed the application of principal component analysis (PCA) for the purpose of dimensionality reduction. Participants also underwent the Test of Attentional Performance (TAP), which assessed their capacity for sustained attention; the Trail Making Test (TMT), which measures cognitive flexibility; the Vocabulary Test (WST), which indicates the measurement of verbal intelligence level and the assessment of language comprehension; and the LPS-2, which measures logical or inferential thinking and quantifies fluid intelligence. We divided the test results of the TAP, TMT, WST, and LPS-2 into two categories: high scoring group and low scoring group, which served as indicators to measure the effectiveness of the model. To enable comprehensive and equitable benchmarking against existing approaches, we introduce commonly used small-scale synchronized datasets named CN-EPFL dataset [20] with 20 individuals. Further details on datase tand Pre-processing can be found in Supplementary Material.

4.2 Implementation Details for Experiment

We validated the performance of our model by differentiating high scoring group and low scoring group. The 5-fold cross-validation (CV) scheme was used to obtain a reliable evaluation on the performance of competing models and the proposed FE-NET. Classification performance was assessed using multiple metrics, including classification accuracy (Acc), precision (Pre), and specificity (Spe).

For dynamic fMRI-EEG hypergraphs embedding module, the α_e and α_e is set as 0.05 and 0.9, the learning rate we set is 10^{-2}, weight decay we set is 5×10^{-4}, the dropout we used is 0.2, we use 5 multi-layer Interactive Hyperedge Neurons modules to form the generator for fMRI -EEG hypergraphs, and the η is we set is 0.6. The parameter settings and introductions of competing models are shown in Supplementary Material.

Table 1: Comparing FE-NET's performance (average accuracy±standard deviation) with other state-of-the-art methods

TAP-WST	Method	Acc	Pre	Spe	TMT-LPS	Acc	Pre	Spe
	BrainGNN [21]	67.23±2.15	71.89±6.42	70.59±3.17		61.38±3.27	60.54±3.85	61.27±4.36
	M-GAT-BC [22]	70.19±4.82	70.57±5.03	65.39±4.21		60.83±7.61	65.71±6.92	62.83±2.49
High	SGP-SL [23]	55.62±4.17	59.48±4.76	56.29±6.84	High	59.35±3.24	61.09±5.73	57.92±3.18
Sustained	Cross-GNN [24]	74.83±5.29	71.06±5.47	74.35±4.82	Cognitive	68.57±3.63	63.82±5.49	62.45±3.71
Attention:	TAN [25]:	73.12±5.37	70.49±3.85	71.84±4.93	Flexibility	68.29±6.83	66.71±5.03	63.62±3.47
VS.	RH-BrainFS [26]	74.26±5.13	71.93±4.58	73.74±3.81	VS.	61.29±3.51	66.38±4.27	66.54±5.18
Low	MCRLN [27]	65.71±4.53	70.28±2.94	69.83±6.21	Low	66.47±5.76	61.73±4.62	62.84±3.49
Sustained	MMP-GCN [28]	79.42±5.19	70.58±5.49	71.95±3.27	Cognitive	66.29±6.83	68.37±5.68	61.93±7.84
Attention	FE-NET	**85.29±2.57**	**83.46±3.19**	**80.83±4.05**	Flexibility	**79.18±3.47**	**75.29±4.83**	**74.38±5.62**
	FE-NETnoFEH	78.45±3.82	78.63±2.47	72.91±2.73		73.57±3.64	69.27±4.18	66.84±3.59
	FE-NETnoFED	79.35±2.67	80.17±5.83	76.82±6.45		70.46±8.53	67.38±5.29	67.49±5.84
	BrainGNN [21]	65.93±3.74	68.27±4.85	67.38±3.29		60.84±4.57	61.29±3.87	60.93±4.18
	M-GAT-BC [22]	68.53±3.18	69.47±4.63	64.72±3.85		62.38±4.19	64.59±5.47	61.73±2.94
High	SGP-SL [23]	56.84±4.73	60.38±4.19	58.62±5.84	High	59.47±3.29	61.83±5.29	57.46±3.85
Verbal	Cross-GNN [24]	72.59±5.47	69.84±5.18	73.27±4.73	Logical	68.29±3.58	63.47±5.39	62.84±3.29
Intelligence	TAN [25]:	71.38±4.85	67.29±3.18	69.47±4.29	Intelligence	68.53±6.47	66.82±5.84	63.19±3.47
VS.	RH-BrainFS [26]	73.62±4.18	68.53±4.73	72.84±3.85	VS.	61.29±3.47	66.38±4.29	66.47±5.18
Low	MCRLN [27]	64.82±4.73	69.47±2.85	68.29±6.47	Low	66.53±5.29	61.84±4.18	62.38±3.19
Verbal	MMP-GCN [28]	77.29±5.84	68.53±5.47	70.38±3.19	Logical	66.84±6.73	68.29±5.39	61.47±7.47
Intelligence	FE-NET	**82.19±2.84**	**80.47±3.85**	**78.53±4.73**	Intelligence	**77.38±3.47**	**73.29±4.85**	**72.84±5.47**
	FE-NETnoFEH	78.29±3.85	77.38±2.84	73.62±2.47		73.47±3.29	69.53±4.18	66.29±3.85
	FE-NETnoFED	79.84±2.73	79.62±5.29	75.47±6.18		70.53±8.47	67.38±5.84	67.29±5.47

4.3 Overall Evaluation

These competing methods and our FE-NET can be categorized into two groups: (Group A): fMRI or EEG modeling method including BrainGNN, M-GAT-BC, and SGP-SL. (Group B): Multimodal brain imaging modeling method including Cross-GNN, TAN, RH-BrainFS, MCRLN, and MMP-GCN.

As shown in Table 1, on one hand, the proposed FE-NET generally significantly outperforms three single-modal brain imaging modeling methods in four different tasks by a large margin, which substantiates the effectiveness of the fusion between fMRI and EEG.

On the other hand, compared with five multimodal brain imaging modeling methods, our FE-NET yields consistently better results in all metrics, Cross-GNN aimed at capturing inter-modal dependencies through dynamic graph learning and mutual learning mechanisms. Specifically, the inter-modal representations are carefully coupled into the combined space to infer the dependencies between modalities. However, Cross-GNN can not eliminate complex data distribution between fMRI and EEG. In contrast, our approach successfully narrow the gap between the hemodynamic responses and the neural oscillations through synchronization operation of GAN-based OFEI and IHEN.

TAN introduces a triple network to extract discriminative information from the high-order representation feature space obtained from multi-modal data. It incorporates self-attention to dynamically estimate the importance of brain regions and utilizes the cross-attention mechanism to extract complementary information from different modalities. However, TAN overlooks the absence of a one-to-one correspondence between fMRI and EEG and used static systems, resulting in the loss of complementary information between the two modalities. In contrast, our method depict the continuous dynamics of hidden representation by Neural ODEs, thereby capturing this relationship.

Generalization capability evaluation: To further evaluate our generalization capability, we conducted additional benchmarking on the synchronized CN-EPFL datasets. The result is shown in

Supplementary Material, all methods were trained on LEMON and tested on CN-EPFL, all models were both trained and tested on CN-EPFL. The results demonstrate that our model still exhibits significant advantages, whether generalizing to task-related datasets or directly utilizing synchronized datasets, further validating its superiority.

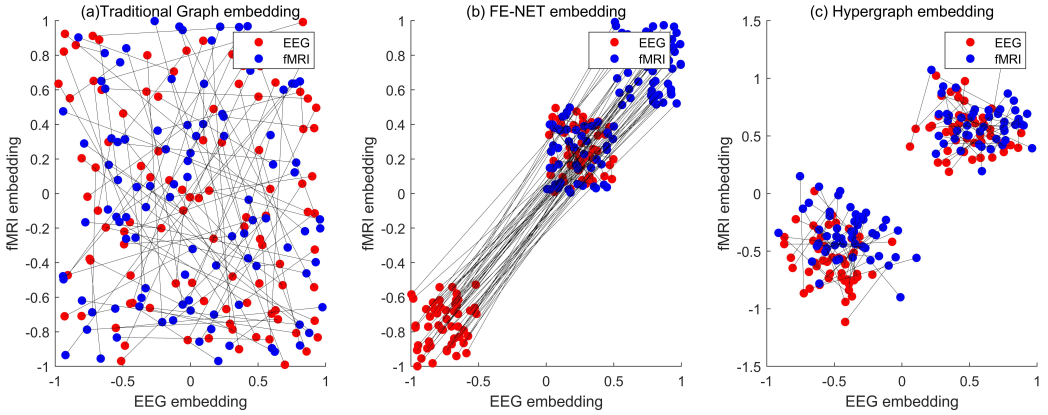

Figure 2: Visualization of the modality gap between the EEG and fMRI modalities.

4.4 FED, and FEH Modules Analysis

As shown in Table 1, we conducted ablation experiments on FED and FEH modules, FE-NETnoFEH and FE-NETnoFED are variants of FE-NET. FE-NETnoFEH employs initial hypergraphs generated by DHC algorithm as inputs for the FED module, whereas FE-NETnoFED utilizes a traditional hypergraph neural network for graph embedding. The superior performance of FE-NET compared to these two variants demonstrates the effectiveness of the modules we proposed. We have attempted to use traditional methods to model the process of transitioning from $x(t_k)$ to $x(t_{k+1})$. As shown in Supplementary Material, the performance of FE-NET (RNN, LSTM, GRU) is not as effective as FE-NET.

The ablation study of OFEI and IHEN in FEH is conducted by evaluating the average accuracy in four downstream tasks. The result is shown in the Supplementary Material. The variants of FED that exclusively employ OFEI or IHEN are referred to as "FEH(OFEI)" and "FEH(IHEN)", respectively. The performance of FEH outperforms "FEH(OFEI)" and "FEH(IHEN)", demonstrating its effectiveness. Additionally, the efficacy of the control and diffusion processes within the FED is validated. The variants of FED that employ exclusively control processes or diffusion processes are denoted as "FED(Con)" and "FED(Diff)" respectively. A comparative analysis of the two processes reveals that the inclusion of only the control process or diffusion process, which relies solely on initial vertex features and neglects the hypergraph structure, results in inferior outcomes. We provided an algorithm complexity and computation resources analysis of FEH-FED and comparison of computational resources with other SOTA methods in the Supplementary Material.

Modality embedding space analysis: As demonstrated in [29], a modality gap exists within multimodal learning, wherein information from different modalities is situated in entirely distinct embedding spaces. This modality gap is correlated with model performance.

To gain a deeper understanding of the performance improvements attributed to the proposed Neural ODEs-based hypergraph strategy, we present a visualization of the modality gap between the EEG and fMRI modalities within the LEMON dataset as shown in Figure 2. A comparison of FE-NET with the hypergraph and traditional graph embedding reveals that traditional graph embedding results in a larger modality gap, which in turn leads to decreased performance. Meanwhile, compared to hypergraph embedding, FE-NET enhances the clustering of embeddings between EEG and fMRI modalities in the embedding space. Notably, the embedding spaces of certain ROI in fMRI are relatively close to each other in Figure 2 (b) when compared to hypergraph embedding in Figure 2 (c). Multiple studies suggest that some ROI of fMRI show a strong correlation with EEG[30], whereas some show no significant association. These observations provide interpretability for the superior performance of Neural ODEs-based hypergraphs in FE-NET.

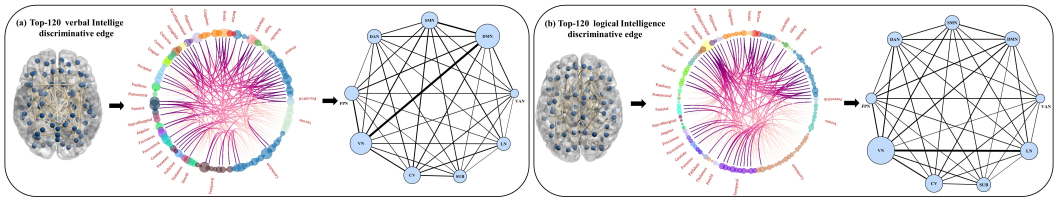

Figure 3: Functional connectivity of verbal intelligence and logical intelligence networks analysis

4.5 Functional connectivity networks analysis

To identify which FC are most discriminative, we use the method described in the literature [31] to rank the important Hyperedges. We summarize the top-120 verbal intelligence and logical intelligence discriminative FC and visualize them for analysis in Figure 3. The FC associated with verbal intelligence, as shown in Figure 3(a), exhibits the highest scores predominantly within the Default Mode Network (DMN), a fundamental FC network consistently identified in fMRI studies [32]. Within the DMN, the FCs demonstrating the strongest predictive capacity are primarily localized in the dorsal anterior cingulate cortex and the posterior superior temporal cortex. These regions, positioned at the intersection of the frontal and temporal lobes, constitute key components of the theory of mind network. In contrast, as shown in Figure 3(b), the FC most strongly associated with logical intelligence is primarily situated within the VN. Furthermore, the verbal intelligence-related FC in Figure 3(a) associated with the posterior superior temporal cortex has been ascertained to possess a reliable predictive value within the Ventral Attention Network (VAN) [33]. The FCs with the highest efficacy are located in the parahippocampal gyrus, and superior parietal lobule [34].

5 Conclusion

This paper designed a novel fMRI-EEG modeling method based on Neural ODEs named FE-NET. FE-NET performs substantially better than many state-of-the-art methods. The contributions of our research are as follows:

1) We propose a unified framework with two key components: FEH module and FED module. FEH can synthesize hypergraphs at multiple spatial and temporal scales, allowing the GAN to learn the joint distribution of hemodynamic and neural-oscillation signals and thus narrow the modality gap. FED, by contrast, uses Neural ODEs to capture latent temporal dependencies, inherently reconciling inconsistent sampling rates and temporal misalignment through learned differential equations governing asynchronous data dynamics.

2) For the first time, we attempt to model asynchronous fMRI and EEG data as Neural ODEs based hypergraph. Compared to previous studies that relied on tiny-sized synchronized datasets, the robustness and practicality of our model are further ensured.

Extensive comparative experiments and ablation studies validate the effectiveness of our proposed model and the corresponding two modules. Meanwhile, compared to simultaneously recorded fMRI-EEG data, asynchronously acquired single modality of EEG data is significantly less costly, which demonstrates the practical applicability of our method.

6 Acknowledgements

We would like to thank the reviewers and the chairs for their suggestions and efforts.

References

[1] S. M. Plis, D. R. Hjelm, R. Salakhutdinov, E. A. Allen, H. J. Bockholt, J. D. Long, H. J. Johnson, J. S. Paulsen, J. A. Turner, and V. D. Calhoun, "Deep learning for neuroimaging: a validation study," *Frontiers in neuroscience*, vol. 8, p. 229, 2014.

[2] Y. Ma, Q. Wang, L. Cao, L. Li, C. Zhang, L. Qiao, and M. Liu, "Multi-scale dynamic graph learning for brain disorder detection with functional mri," *IEEE Transactions on Neural Systems and Rehabilitation Engineering*, vol. 31, no. 42, pp. 3501–3512, 2023.

[3] J. Kawahara, C. J. Brown, S. P. Miller, B. G. Booth, V. Chau, R. E. Grunau, J. G. Zwicker, and G. Hamarneh, "Brainnetcnn: Convolutional neural networks for brain networks; towards predicting neurodevelopment," *NeuroImage*, vol. 146, pp. 1038–1049, 2017.

[4] Z. Jia, Y. Lin, J. Wang, R. Zhou, X. Ning, Y. He, and Y. Zhao, "Graphsleepnet: Adaptive spatial-temporal graph convolutional networks for sleep stage classification." in *Ijcai*, vol. 2021, 2020, pp. 1324–1330.

[5] W. B. Bruin, L. Taylor, R. M. Thomas, J. P. Shock, P. Zhutovsky, Y. Abe, P. Alonso, S. H. Ameis, A. Anticevic, P. D. Arnold *et al.*, "Structural neuroimaging biomarkers for obsessive-compulsive disorder in the enigma-ocd consortium: medication matters," *Translational psychiatry*, vol. 10, no. 1, p. 342, 2020.

[6] R. M. Cichy and A. Oliva, "Am/eeg-fmri fusion primer: resolving human brain responses in space and time," *Neuron*, vol. 107, no. 5, pp. 772–781, 2020.

[7] R. T. Chen, Y. Rubanova, J. Bettencourt, and D. K. Duvenaud, "Neural ordinary differential equations," *Advances in neural information processing systems*, vol. 31, 2018.

[8] Y. Sun, L. Zhang, and H. Schaeffer, "Neupde: Neural network based ordinary and partial differential equations for modeling time-dependent data," in *Mathematical and Scientific Machine Learning*. PMLR, 2020, pp. 352–372.

[9] D. Zhou, J. Huang, and B. Schölkopf, "Learning with hypergraphs: Clustering, classification, and embedding," *Advances in neural information processing systems*, vol. 19, 2006.

[10] Y. Feng, H. You, Z. Zhang, R. Ji, and Y. Gao, "Hypergraph neural networks," in *Proceedings of the AAAI conference on artificial intelligence*, vol. 33, no. 01, 2019, pp. 3558–3565.

[11] S. Bai, F. Zhang, and P. H. Torr, "Hypergraph convolution and hypergraph attention," *Pattern Recognition*, vol. 110, p. 107637, 2021.

[12] P. Veličković, G. Cucurull, A. Casanova, A. Romero, P. Lio, and Y. Bengio, "Graph attention networks," *arXiv preprint arXiv:1710.10903*, 2017.

[13] N. Yadati, M. Nimishakavi, P. Yadav, V. Nitin, A. Louis, and P. Talukdar, "Hypergcn: A new method for training graph convolutional networks on hypergraphs," *Advances in neural information processing systems*, vol. 32, 2019.

[14] J. Jiang, Y. Wei, Y. Feng, J. Cao, and Y. Gao, "Dynamic hypergraph neural networks." in *IJCAI*, 2019, pp. 2635–2641.

[15] J. Geiser, *Decomposition methods for differential equations: theory and applications*. CRC Press, 2009.

[16] W. Song, C. Shi, Z. Xiao, Z. Duan, Y. Xu, M. Zhang, and J. Tang, "Autoint: Automatic feature interaction learning via self-attentive neural networks," in *Proceedings of the 28th ACM international conference on information and knowledge management*, 2019, pp. 1161–1170.

[17] P. Zhou, W. Shi, J. Tian, Z. Qi, B. Li, H. Hao, and B. Xu, "Attention-based bidirectional long short-term memory networks for relation classification," in *Proceedings of the 54th Annual Meeting of the Association for Computational Linguistics (Volume 2: Short Papers)*, K. Erk and N. A. Smith, Eds. Berlin, Germany: Association for Computational Linguistics, Aug. 2016, pp. 207–212. [Online]. Available: https://aclanthology.org/P16-2034

[18] A. Babayan, M. Erbey, D. Kumral, J. D. Reinelt, A. M. Reiter, J. Röbbig, H. L. Schaare, M. Uhlig, A. Anwander, P.-L. Bazin *et al.*, "A mind-brain-body dataset of mri, eeg, cognition, emotion, and peripheral physiology in young and old adults," *Scientific data*, vol. 6, no. 1, pp. 1–21, 2019.

[19] A. Delorme and S. Makeig, "Eeglab: an open source toolbox for analysis of single-trial eeg dynamics including independent component analysis," *Journal of neuroscience methods*, vol. 134, no. 1, pp. 9–21, 2004.

[20] M. Pereira, N. Faivre, I. Iturrate, M. Wirthlin, L. Serafini, S. Martin, A. Desvachez, O. Blanke, D. Van De Ville, and J. d. R. Millán, "Disentangling the origins of confidence in speeded perceptual judgments through multimodal imaging," *Proceedings of the National Academy of Sciences*, vol. 117, no. 15, pp. 8382–8390, 2020.

[21] X. Li, Y. Zhou, N. Dvornek, M. Zhang, S. Gao, J. Zhuang, D. Scheinost, L. H. Staib, P. Ventola, and J. S. Duncan, "Braingnn: Interpretable brain graph neural network for fmri analysis," *Medical Image Analysis*, vol. 74, p. 102233, 2021.

[22] R. Yu, C. Pan, X. Fei, M. Chen, and D. Shen, "Multi-graph attention networks with bilinear convolution for diagnosis of schizophrenia," *IEEE Journal of Biomedical and Health Informatics*, vol. 27, no. 3, pp. 1443–1454, 2023.

[23] T. Chen, Y. Guo, S. Hao, and R. Hong, "Exploring self-attention graph pooling with eeg-based topological structure and soft label for depression detection," *IEEE transactions on affective computing*, vol. 13, no. 4, pp. 2106–2118, 2022.

[24] Y. Yang, C. Ye, X. Guo, T. Wu, Y. Xiang, and T. Ma, "Mapping multi-modal brain connectome for brain disorder diagnosis via cross-modal mutual learning," *IEEE Transactions on Medical Imaging*, 2023.

[25] Q. Zhu, H. Wang, B. Xu, Z. Zhang, W. Shao, and D. Zhang, "Multimodal triplet attention network for brain disease diagnosis," *IEEE Transactions on Medical Imaging*, vol. 41, no. 12, pp. 3884–3894, 2022.

[26] H. Ye, Y. Zheng, Y. Li, K. Zhang, Y. Kong, and Y. Yuan, "Rh-brainfs: Regional heterogeneous multimodal brain networks fusion strategy," *Advances in Neural Information Processing Systems*, vol. 36, 2024.

[27] Y. Kong, W. Wang, X. Liu, S. Gao, Z. Hou, C. Xie, Z. Zhang, and Y. Yuan, "Multi-connectivity representation learning network for major depressive disorder diagnosis," *IEEE Transactions on Medical Imaging*, 2023.

[28] X. Song, F. Zhou, A. F. Frangi, J. Cao, X. Xiao, Y. Lei, T. Wang, and B. Lei, "Multicenter and multichannel pooling gcn for early ad diagnosis based on dual-modality fused brain network," *IEEE Transactions on Medical Imaging*, vol. 42, no. 2, pp. 354–367, 2023.

[29] V. W. Liang, Y. Zhang, Y. Kwon, S. Yeung, and J. Y. Zou, "Mind the gap: Understanding the modality gap in multi-modal contrastive representation learning," *Advances in Neural Information Processing Systems*, vol. 35, pp. 17 612–17 625, 2022.

[30] T. Nazneen, I. B. Islam, M. S. R. Sajal, W. Jamal, M. A. Amin, R. Vaidyanathan, T. Chau, and K. A. Mamun, "Recent trends in non-invasive neural recording based brain-to-brain synchrony analysis on multidisciplinary human interactions for understanding brain dynamics: a systematic review," *Frontiers in Computational Neuroscience*, vol. 16, p. 875282, 2022.

[31] J. Liu, W. Cui, Y. Chen, Y. Ma, Q. Dong, R. Cai, Y. Li, and B. Hu, "Deep fusion of multi-template using spatio-temporal weighted multi-hypergraph convolutional networks for brain disease analysis," *IEEE Transactions on Medical Imaging*, 2023.

[32] L. Naci, A. Haugg, A. MacDonald, M. Anello, E. Houldin, S. Naqshbandi, L. E. Gonzalez-Lara, M. Arango, C. Harle, R. Cusack *et al.*, "Functional diversity of brain networks supports consciousness and verbal intelligence," *Scientific reports*, vol. 8, no. 1, p. 13259, 2018.

[33] E. Dryburgh, S. McKenna, and I. Rekik, "Predicting full-scale and verbal intelligence scores from functional connectomic data in individuals with autism spectrum disorder," *Brain imaging and behavior*, vol. 14, no. 5, pp. 1769–1778, 2020.

[34] N. He and C. Kou, "Prediction of individual performance and verbal intelligence scores from resting-state fmri in children and adolescents," *International Journal of Developmental Neuroscience*, vol. 84, no. 7, pp. 779–790, 2024.

NeurIPS Paper Checklist

1. **Claims**

   Question: Do the main claims made in the abstract and introduction accurately reflect the paper's contributions and scope?

   Answer: [Yes]

   Justification: accurately reflect

   Guidelines:

   - The answer NA means that the abstract and introduction do not include the claims made in the paper.
   - The abstract and/or introduction should clearly state the claims made, including the contributions made in the paper and important assumptions and limitations. A No or NA answer to this question will not be perceived well by the reviewers.
   - The claims made should match theoretical and experimental results, and reflect how much the results can be expected to generalize to other settings.
   - It is fine to include aspirational goals as motivation as long as it is clear that these goals are not attained by the paper.

2. **Limitations**

   Question: Does the paper discuss the limitations of the work performed by the authors?

   Answer: [No]

   Justification: limited pages

   Guidelines:

   - The answer NA means that the paper has no limitation while the answer No means that the paper has limitations, but those are not discussed in the paper.
   - The authors are encouraged to create a separate "Limitations" section in their paper.
   - The paper should point out any strong assumptions and how robust the results are to violations of these assumptions (e.g., independence assumptions, noiseless settings, model well-specification, asymptotic approximations only holding locally). The authors should reflect on how these assumptions might be violated in practice and what the implications would be.
   - The authors should reflect on the scope of the claims made, e.g., if the approach was only tested on a few datasets or with a few runs. In general, empirical results often depend on implicit assumptions, which should be articulated.
   - The authors should reflect on the factors that influence the performance of the approach. For example, a facial recognition algorithm may perform poorly when image resolution is low or images are taken in low lighting. Or a speech-to-text system might not be used reliably to provide closed captions for online lectures because it fails to handle technical jargon.
   - The authors should discuss the computational efficiency of the proposed algorithms and how they scale with dataset size.
   - If applicable, the authors should discuss possible limitations of their approach to address problems of privacy and fairness.
   - While the authors might fear that complete honesty about limitations might be used by reviewers as grounds for rejection, a worse outcome might be that reviewers discover limitations that aren't acknowledged in the paper. The authors should use their best judgment and recognize that individual actions in favor of transparency play an important role in developing norms that preserve the integrity of the community. Reviewers will be specifically instructed to not penalize honesty concerning limitations.

3. **Theory assumptions and proofs**

   Question: For each theoretical result, does the paper provide the full set of assumptions and a complete (and correct) proof?

   Answer: [No]

Justification: limited pages

Guidelines:

- The answer NA means that the paper does not include theoretical results.
- All the theorems, formulas, and proofs in the paper should be numbered and cross-referenced.
- All assumptions should be clearly stated or referenced in the statement of any theorems.
- The proofs can either appear in the main paper or the supplemental material, but if they appear in the supplemental material, the authors are encouraged to provide a short proof sketch to provide intuition.
- Inversely, any informal proof provided in the core of the paper should be complemented by formal proofs provided in appendix or supplemental material.
- Theorems and Lemmas that the proof relies upon should be properly referenced.

4. **Experimental result reproducibility**

   Question: Does the paper fully disclose all the information needed to reproduce the main experimental results of the paper to the extent that it affects the main claims and/or conclusions of the paper (regardless of whether the code and data are provided or not)?

   Answer:[Yes]

   Justification: code will provided

   Guidelines:

   - The answer NA means that the paper does not include experiments.
   - If the paper includes experiments, a No answer to this question will not be perceived well by the reviewers: Making the paper reproducible is important, regardless of whether the code and data are provided or not.
   - If the contribution is a dataset and/or model, the authors should describe the steps taken to make their results reproducible or verifiable.
   - Depending on the contribution, reproducibility can be accomplished in various ways. For example, if the contribution is a novel architecture, describing the architecture fully might suffice, or if the contribution is a specific model and empirical evaluation, it may be necessary to either make it possible for others to replicate the model with the same dataset, or provide access to the model. In general. releasing code and data is often one good way to accomplish this, but reproducibility can also be provided via detailed instructions for how to replicate the results, access to a hosted model (e.g., in the case of a large language model), releasing of a model checkpoint, or other means that are appropriate to the research performed.
   - While NeurIPS does not require releasing code, the conference does require all submissions to provide some reasonable avenue for reproducibility, which may depend on the nature of the contribution. For example
     (a) If the contribution is primarily a new algorithm, the paper should make it clear how to reproduce that algorithm.
     (b) If the contribution is primarily a new model architecture, the paper should describe the architecture clearly and fully.
     (c) If the contribution is a new model (e.g., a large language model), then there should either be a way to access this model for reproducing the results or a way to reproduce the model (e.g., with an open-source dataset or instructions for how to construct the dataset).
     (d) We recognize that reproducibility may be tricky in some cases, in which case authors are welcome to describe the particular way they provide for reproducibility. In the case of closed-source models, it may be that access to the model is limited in some way (e.g., to registered users), but it should be possible for other researchers to have some path to reproducing or verifying the results.

5. **Open access to data and code**

   Question: Does the paper provide open access to the data and code, with sufficient instructions to faithfully reproduce the main experimental results, as described in supplemental material?

Answer: [No]

Justification: code will be provided

Guidelines:

- The answer NA means that paper does not include experiments requiring code.
- Please see the NeurIPS code and data submission guidelines (`https://nips.cc/public/guides/CodeSubmissionPolicy`) for more details.
- While we encourage the release of code and data, we understand that this might not be possible, so "No" is an acceptable answer. Papers cannot be rejected simply for not including code, unless this is central to the contribution (e.g., for a new open-source benchmark).
- The instructions should contain the exact command and environment needed to run to reproduce the results. See the NeurIPS code and data submission guidelines (`https://nips.cc/public/guides/CodeSubmissionPolicy`) for more details.
- The authors should provide instructions on data access and preparation, including how to access the raw data, preprocessed data, intermediate data, and generated data, etc.
- The authors should provide scripts to reproduce all experimental results for the new proposed method and baselines. If only a subset of experiments are reproducible, they should state which ones are omitted from the script and why.
- At submission time, to preserve anonymity, the authors should release anonymized versions (if applicable).
- Providing as much information as possible in supplemental material (appended to the paper) is recommended, but including URLs to data and code is permitted.

6. **Experimental setting/details**

   Question: Does the paper specify all the training and test details (e.g., data splits, hyperparameters, how they were chosen, type of optimizer, etc.) necessary to understand the results?

   Answer: [Yes]

   Justification: Can be find in Implementation Details for Experiment section

   Guidelines:

   - The answer NA means that the paper does not include experiments.
   - The experimental setting should be presented in the core of the paper to a level of detail that is necessary to appreciate the results and make sense of them.
   - The full details can be provided either with the code, in appendix, or as supplemental material.

7. **Experiment statistical significance**

   Question: Does the paper report error bars suitably and correctly defined or other appropriate information about the statistical significance of the experiments?

   Answer: [Yes]

   Justification: Can be find in Overall Evaluation section

   Guidelines:

   - The answer NA means that the paper does not include experiments.
   - The authors should answer "Yes" if the results are accompanied by error bars, confidence intervals, or statistical significance tests, at least for the experiments that support the main claims of the paper.
   - The factors of variability that the error bars are capturing should be clearly stated (for example, train/test split, initialization, random drawing of some parameter, or overall run with given experimental conditions).
   - The method for calculating the error bars should be explained (closed form formula, call to a library function, bootstrap, etc.)
   - The assumptions made should be given (e.g., Normally distributed errors).
   - It should be clear whether the error bar is the standard deviation or the standard error of the mean.

- It is OK to report 1-sigma error bars, but one should state it. The authors should preferably report a 2-sigma error bar than state that they have a 96% CI, if the hypothesis of Normality of errors is not verified.
- For asymmetric distributions, the authors should be careful not to show in tables or figures symmetric error bars that would yield results that are out of range (e.g. negative error rates).
- If error bars are reported in tables or plots, The authors should explain in the text how they were calculated and reference the corresponding figures or tables in the text.

8. **Experiments compute resources**

   Question: For each experiment, does the paper provide sufficient information on the computer resources (type of compute workers, memory, time of execution) needed to reproduce the experiments?

   Answer: [No]

   Justification: limited pages

   Guidelines:

   - The answer NA means that the paper does not include experiments.
   - The paper should indicate the type of compute workers CPU or GPU, internal cluster, or cloud provider, including relevant memory and storage.
   - The paper should provide the amount of compute required for each of the individual experimental runs as well as estimate the total compute.
   - The paper should disclose whether the full research project required more compute than the experiments reported in the paper (e.g., preliminary or failed experiments that didn't make it into the paper).

9. **Code of ethics**

   Question: Does the research conducted in the paper conform, in every respect, with the NeurIPS Code of Ethics `https://neurips.cc/public/EthicsGuidelines`?

   Answer: [Yes]

   Justification:

   Guidelines:

   - The answer NA means that the authors have not reviewed the NeurIPS Code of Ethics.
   - If the authors answer No, they should explain the special circumstances that require a deviation from the Code of Ethics.
   - The authors should make sure to preserve anonymity (e.g., if there is a special consideration due to laws or regulations in their jurisdiction).

10. **Broader impacts**

    Question: Does the paper discuss both potential positive societal impacts and negative societal impacts of the work performed?

    Answer: [Yes]

    Justification: in conclusion section

    Guidelines:

    - The answer NA means that there is no societal impact of the work performed.
    - If the authors answer NA or No, they should explain why their work has no societal impact or why the paper does not address societal impact.
    - Examples of negative societal impacts include potential malicious or unintended uses (e.g., disinformation, generating fake profiles, surveillance), fairness considerations (e.g., deployment of technologies that could make decisions that unfairly impact specific groups), privacy considerations, and security considerations.
    - The conference expects that many papers will be foundational research and not tied to particular applications, let alone deployments. However, if there is a direct path to any negative applications, the authors should point it out. For example, it is legitimate to point out that an improvement in the quality of generative models could be used to

generate deepfakes for disinformation. On the other hand, it is not needed to point out that a generic algorithm for optimizing neural networks could enable people to train models that generate Deepfakes faster.

- The authors should consider possible harms that could arise when the technology is being used as intended and functioning correctly, harms that could arise when the technology is being used as intended but gives incorrect results, and harms following from (intentional or unintentional) misuse of the technology.
- If there are negative societal impacts, the authors could also discuss possible mitigation strategies (e.g., gated release of models, providing defenses in addition to attacks, mechanisms for monitoring misuse, mechanisms to monitor how a system learns from feedback over time, improving the efficiency and accessibility of ML).

11. **Safeguards**

    Question: Does the paper describe safeguards that have been put in place for responsible release of data or models that have a high risk for misuse (e.g., pretrained language models, image generators, or scraped datasets)?

    Answer:[Yes]

    Justification:

    Guidelines:

    - The answer NA means that the paper poses no such risks.
    - Released models that have a high risk for misuse or dual-use should be released with necessary safeguards to allow for controlled use of the model, for example by requiring that users adhere to usage guidelines or restrictions to access the model or implementing safety filters.
    - Datasets that have been scraped from the Internet could pose safety risks. The authors should describe how they avoided releasing unsafe images.
    - We recognize that providing effective safeguards is challenging, and many papers do not require this, but we encourage authors to take this into account and make a best faith effort.

12. **Licenses for existing assets**

    Question: Are the creators or original owners of assets (e.g., code, data, models), used in the paper, properly credited and are the license and terms of use explicitly mentioned and properly respected?

    Answer: [Yes]

    Justification:

    Guidelines:

    - The answer NA means that the paper does not use existing assets.
    - The authors should cite the original paper that produced the code package or dataset.
    - The authors should state which version of the asset is used and, if possible, include a URL.
    - The name of the license (e.g., CC-BY 4.0) should be included for each asset.
    - For scraped data from a particular source (e.g., website), the copyright and terms of service of that source should be provided.
    - If assets are released, the license, copyright information, and terms of use in the package should be provided. For popular datasets, `paperswithcode.com/datasets` has curated licenses for some datasets. Their licensing guide can help determine the license of a dataset.
    - For existing datasets that are re-packaged, both the original license and the license of the derived asset (if it has changed) should be provided.
    - If this information is not available online, the authors are encouraged to reach out to the asset's creators.

13. **New assets**

    Question: Are new assets introduced in the paper well documented and is the documentation provided alongside the assets?

Answer: [No]

Justification:

Guidelines:

- The answer NA means that the paper does not release new assets.
- Researchers should communicate the details of the dataset/code/model as part of their submissions via structured templates. This includes details about training, license, limitations, etc.
- The paper should discuss whether and how consent was obtained from people whose asset is used.
- At submission time, remember to anonymize your assets (if applicable). You can either create an anonymized URL or include an anonymized zip file.

14. **Crowdsourcing and research with human subjects**

    Question: For crowdsourcing experiments and research with human subjects, does the paper include the full text of instructions given to participants and screenshots, if applicable, as well as details about compensation (if any)?

    Answer: [No]

    Justification:

    Guidelines:

    - The answer NA means that the paper does not involve crowdsourcing nor research with human subjects.
    - Including this information in the supplemental material is fine, but if the main contribution of the paper involves human subjects, then as much detail as possible should be included in the main paper.
    - According to the NeurIPS Code of Ethics, workers involved in data collection, curation, or other labor should be paid at least the minimum wage in the country of the data collector.

15. **Institutional review board (IRB) approvals or equivalent for research with human subjects**

    Question: Does the paper describe potential risks incurred by study participants, whether such risks were disclosed to the subjects, and whether Institutional Review Board (IRB) approvals (or an equivalent approval/review based on the requirements of your country or institution) were obtained?

    Answer: [No]

    Justification:

    Guidelines:

    - The answer NA means that the paper does not involve crowdsourcing nor research with human subjects.
    - Depending on the country in which research is conducted, IRB approval (or equivalent) may be required for any human subjects research. If you obtained IRB approval, you should clearly state this in the paper.
    - We recognize that the procedures for this may vary significantly between institutions and locations, and we expect authors to adhere to the NeurIPS Code of Ethics and the guidelines for their institution.
    - For initial submissions, do not include any information that would break anonymity (if applicable), such as the institution conducting the review.

16. **Declaration of LLM usage**

    Question: Does the paper describe the usage of LLMs if it is an important, original, or non-standard component of the core methods in this research? Note that if the LLM is used only for writing, editing, or formatting purposes and does not impact the core methodology, scientific rigorousness, or originality of the research, declaration is not required.

    Answer: [NA] .

Justification:

Guidelines:

- The answer NA means that the core method development in this research does not involve LLMs as any important, original, or non-standard components.
- Please refer to our LLM policy (`https://neurips.cc/Conferences/2025/LLM`) for what should or should not be described.

A Technical Appendices

All additional results can be downloaded and found in the supplementary material.